

# Coronary Characterization in Multi-slice Computed Tomography

C Toumoulin<sup>1</sup>, C Boldak<sup>2</sup>, M Garreau<sup>1</sup>, D Boulmier<sup>3</sup>

<sup>1</sup>LTSI, INSERM, Université de Rennes 1, Rennes, France

<sup>2</sup>Computer Science Department, Institute of Bialystok, Poland

<sup>3</sup>Service d'hémodynamique et de cardiologie interventionnelle, CHU Rennes, France

## Abstract

*We present a 3D extraction method of coronaries in MSCT, which aims at refining the delineating of the vascular inner wall and the calcified contours for quantification purposes. The proposed approach makes use of a two-step process: the first one performs a vessel central axis tracking by applying a semi-automatic 3D geometrical moment-based method. A refinement is then performed, based on a level set approach, to improve the detection accuracy of both contours and calcifications. The level sets were applied first in 2-D space, independently on each slice, then in 3-D to perform the extraction directly in the volume. A comparison between the 2-D and 3-D procedures is provided in term of quality of delineation.*

## 1. Introduction

The treatments and prevention of the cardio-vascular diseases represent today an important challenge in term of public health. Atherosclerosis is the most important cause of the vascular wall anomalies. It corresponds to a degeneration of the arterial wall, which gives rise to atherosclerotic plaques and involves, at the latest stage of the disease, morphological modifications of the lumen with the formation of stenosis. The heart, the brain and the lower limbs are the privileged target of this vascular disease. Its characterization calls on imaging techniques, which allows displaying the inner vascular wall and measuring its anomalies. Today, the magnetic resonance angiography and the multi-slice computed tomography are two particularly efficient modalities in vascular imaging and extremely promising in cardiac imaging. Nevertheless, lesion quantification needs the development of fast algorithms for the preliminary extraction of the structures. Tools have to allow physicians to work in satisfactory interactivity

conditions and overcome the intra- and inter-observer variability.

We previously designed a semi-automatic method based on geometric moments to process data volumes of size 500 Mbytes (or more) within 10 seconds to 5 minutes (depending on the complexity of the data) on a PC Pentium III 450 MHz, 512 Mb RAM. 3D Geometric moments up to order 2 were used to estimate the local orientation of the vessel and its diameter taking into account the heterogeneity of the intra-vascular and background surroundings [1]. This work was dealt with a clinical evaluation for the coronary extraction and the parietal calcification location in multi-slice computed tomography. The method provided high sensibility and specificity measures in the assessment of the vascular permeability [2].

We completed this process by locally applying a deformable model on the extracted contours in order to get a more precise delineation of the vessel edges and calcifications. In this hybrid approach, the moment-based method allows getting a first, rough but rapid extraction while the level set approach, more time consuming, acts as a refining process by fitting at best, the deformable curves to the real contours. The objective was getting a satisfactory compromise between computational time and extraction accuracy.

This paper is organized as follows: the refining process based on level sets is presented section 2. Section 3 provides qualitative results on pathological vessels and proposes a quantification tool to evaluate the severity of the narrowing in the calcified areas. Section 4 gives concluding remarks and prospects.

## 2. Deformable model: A level set approach

### 2.1. Level set formalism

The level set was developed by Osher and Sethian [3]

and introduced in the medical field by Malladi and al. [4]. The level set method considers the propagation, in time, of a front along its normal direction. This front  $\Gamma(t)$  can be either a curve or a surface depending on the considered space (2D / 3D). The main idea is to embed this front as the zero level of a higher dimension function  $\phi(X, t)$  such as:

$$\Gamma(t) = \{X \in \mathcal{R}^m, m = 2 \text{ or } 3 / \phi(X, t) = 0\} \quad (1)$$

The function  $\phi$  describes a surface defined by  $\phi(X, t) = d(X, \Gamma)$  where  $d(X, \Gamma)$  is the signed Euclidean distance from the point  $X$  to the front  $\Gamma$ . The distance is positive if the point lies outside the front and negative otherwise. The evolution of this front is guided by a partial differential equation expressed as:

$$\phi_t + F|\nabla\phi| = 0 \text{ given } \phi(X, t=0) = 0 \quad (2)$$

where  $F$  is a propagation velocity directed in the normal direction to the front. It depends on local properties of both the front and the image. The numerical scheme uses finite difference approximations for the spatial and temporal derivative:

$$\phi_{ij}^{n+1} = \phi_{ij}^n - \nabla t \cdot F |\nabla_{ij} \phi_{ij}^n| \quad (3)$$

where  $\nabla t$  refers to the time step,  $n$  to the iteration number and  $(i, j)$  to the pixel location if we dealt with curves.

## 2.2. Application to the vascular segmentation

The evolution model used in this work, was derived from the original Malladi formulation [4]:

$$\begin{aligned} \phi_t + F_s (\nu - \varepsilon \kappa) |\nabla\phi| - \beta \nabla P \nabla\phi &= 0 \\ F_s &= 1 / (1 + |\nabla G_\sigma * I(x)|) \\ P &= -|\nabla G_\sigma * I(x)| \end{aligned} \quad (4)$$

$P$  is the negative absolute of the gradient of the convoluted image.  $\nabla P$  corresponds to an attracting force towards the boundaries and allows stabilizing the front once it has reached the image edges.  $\beta$  is a weighting coefficient that controls the intensity of this force. The velocity force includes three components: (1) a stopping term  $F_s$  based on image gradient, (2) a regularization term built from the local curvature of the front  $\kappa$  (the weight given to this force is represented by  $\varepsilon$ ), (3) a driving expansion (deflation) force  $\nu$ , which makes the front shrink or spread out. In our case, we redefined

$F_s$  and  $\nu$  as follows :

$$\begin{aligned} F_s &= 1 / (1 + |\nabla I|^{GP}) \\ \nu &= V_0 * [\max(I - I_{\max}, 0) - \max(I_{\min} - I, 0)] \end{aligned} \quad (5)$$

$[I_{\min}, I_{\max}]$  represents the vessel intensity interval.  $\nu$  is a density dependent function, which characterizes the membership relation of each point to the structure of interest. This function is used to determine the propagation direction of the front (contraction, expansion, no displacement) and reinforce the strength of this force depending on the intensity difference between the considered point and the range bounds:

1. if  $I(X) < I_{\min}$  then  $\nu = -V_0 * (I_{\min} - I)$ . The force is a contraction force whose intensity depends on the difference  $(I_{\min} - I)$ .
2. if  $I(X) > I_{\max}$  then  $\nu = -V_0 * (I - I_{\max})$ . The force is a expansion force whose intensity depends on the difference  $(I - I_{\max})$ .
3. if  $I_{\min} \leq I(X) \leq I_{\max}$  then  $\nu = 0$ . No force is applied.

$V_0$  and  $GP$  are two weighting coefficients. The first one increases the importance given to the force  $\nu$  in particularly difficult topological situations. The second one limits the impact of the stopping force in the noisy region.

## 3. Experimentations

Experiments were conducted on six angio-scanners, acquired on a Siemens Somatom volume zoom 4 detectors. The acquisition protocols were identical with the following acquisition parameters: collimation of 0.6 mm, table displacement of 1.5 mm/rotation, reconstruction increment of 0.6 mm, size of the matrix 512x512 with an average of 350 slices and a pixel size from 0.33x0.33 to 0.4x0.4 mm. The resolution is 8 bits and the slice thickness of 1.25 mm.

These data were acquired on an aged men population having pretty much diffused vascular lesions. When reading axial slices, we observed the presence of (1) a slender distal network, particularly at the postero-lateral left level (bases 4,5,6), (2) thrombosed and calcified aneurysms on the right coronary artery with a partial downstream over taking by a marginal artery and collaterals compensated dilation of the mid left anterior descending artery or LAD (base 3), (3) a stent on the mean segment of the LAD (base 1) and (4), a double transplant respectively mammary on the LAD and venous on the posterior descending artery (base 2). For all these data sets, and for each vascular segment, we applied first the moment-based method to extract the centerline and estimate the diameter at each extracted



central axis points. A first rough estimation of the calcifications was performed at the same time. Extracted vascular trees are shown for two of the data sets (figures 1 and 2)[1].

The first one includes a calcified aneurysm while the second one displays a stent on the mid left anterior descending artery (LAD).

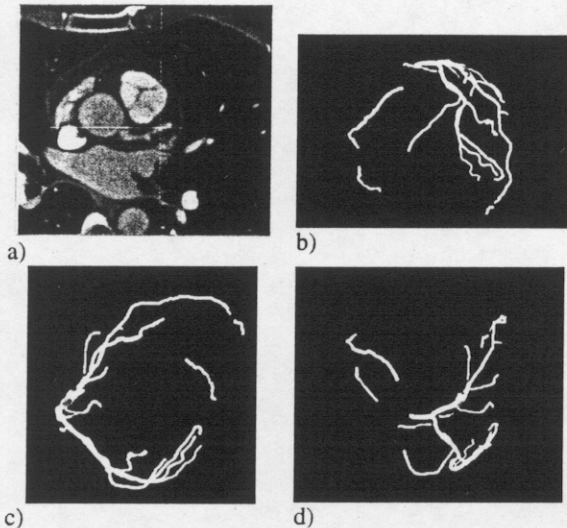


Figure 1: a) a slice in the axial plane of the heart. b-d) MIP projections in the sagittal, axial and coronal planes of the extracted network (including calcification in red on the mid LAD artery)

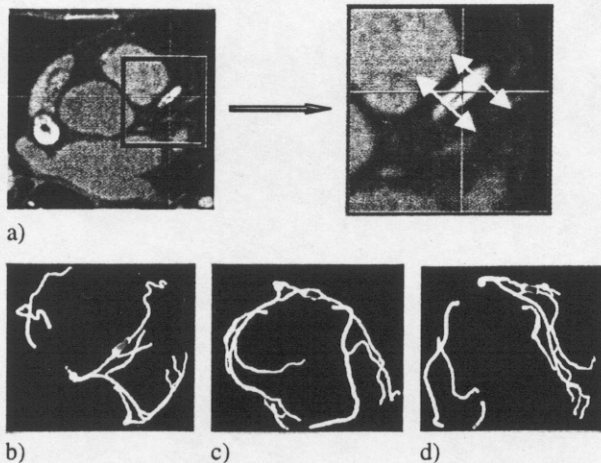


Figure 2: a) a slice in the axial plane at the stent level (green box). The proximal and distal limit of the stent is shown in yellow in the zoomed green box. b-d) MIP projections in the axial, coronal and sagittal planes of the extracted network (including in red the stent on the mid LAD artery)

Two studies were carried out: (1) on the perpendicular slices to the direction of the vessel and centered on each central axis point, (2) in the 3D space by investigating a limited volume around the vessel central axis. The initialization of the zero level front was performed from the contours extracted by the moment-based method. In all cases, a preliminary interpolation (B-spline in 2D/trilinear spline in 3D) was performed between the moment-based extracted central axis points.

Parameters were set with the following values:  $V_0 = 10$ ,  $[I_{min}, I_{max}] = [1100 - 1600]$ ,  $\epsilon = 0$  (no curvature constraints),  $\beta = 0.5$ ,  $GP = 0.5$ .

Figure 3 displays two series of medallions, which represent respectively the results of the 2D and 3D level sets application on a segment of the LAD artery (data set displayed figure 1). In each case (2D and 3D), slices are perpendicular to the direction of the vascular branch. Once the volume is processed, it is visualized using a three-dimensional volume rendering (Figure 3.c). Straight lines, superposed on the 3D reconstructed artery, indicate the position of each slice.

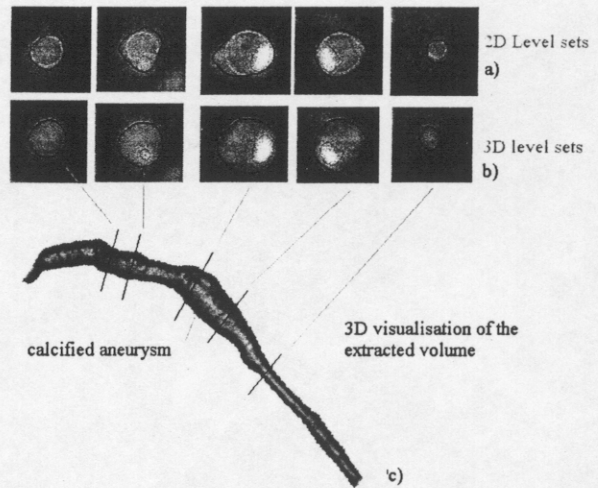


Figure 3: a-b) Results of the extraction (vascular wall in blue and calcification in red) performed in 2D and 3D space (the pink circle represents the vascular wall extracted from the geometric moment-based method). c) 3D visualization of the extracted volume (calcified areas appear in red). The slice locations are depicted by straight lines superposed on the extracted vascular segment.

The calcified aneurysm appears well visible. Its quantification is obtained through a clickable graph (Figure 4) that shows the diameter evolution along the vessel. An interactive inspection of the cross-section along the vessel allows getting different parameters as the aneurysm ratio, the up and downstream mean areas.

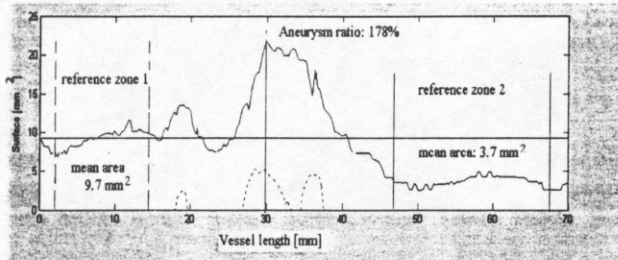


Figure 4: Cross sectional area along the vessel. Solid line: total area including lumen and calcification surface. Dotted line: calcified area. A cursor allows selecting the cross-section of interest and defining the zones that are taken as references to compute the degree of severity of a stenosis or an aneurysm. Here two mean areas were computed up and downstream the aneurysm to help characterizing the severity of the pathology.

Figure 5 displays the results of the 3D level set application on the mean LAD segment where the stent appears. The vascular wall shows the stent impression in the reconstructed volume (in grey level). In this zone, the vessel took the exact shape of the stent. Its diameter is larger and the outer shape well circular. We tried to extract only the stent without taking the vessel in order to check its good unfolding and detect the potential stenosis reformation process.

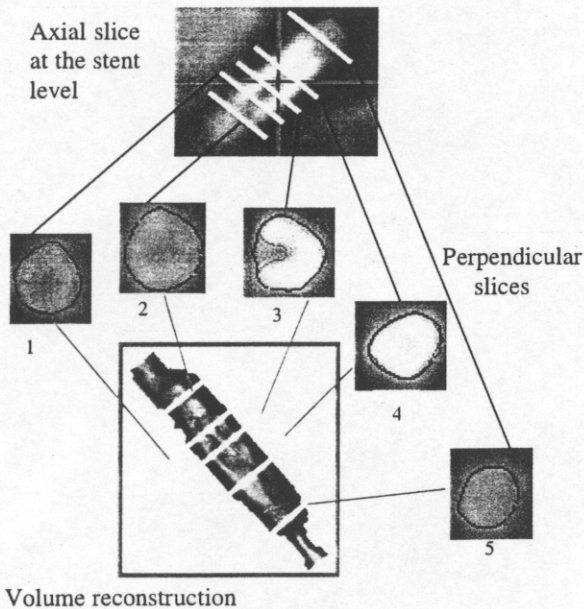


Figure 5: Stent extraction: The stent impression is visible on the 3D reconstructed vascular segment. Results on 2D slices are presented as their location both on the grey level axial slice and the 3D reconstructed volume (red color: stent contour). The delineation of the vascular wall appears in blue on the slices.

The axial slice at the stent level shows a dense mesh and a very thin inner lumen. We should detect two contours: inner and outer, the latter one being identical to the vascular wall's (in blue). The delineation result is shown in red on the 2D slices and the reconstructed volume. The outer contour of this stent is well defined on slice 4 while no inner contour was detected. At this level the density inside the vessel, is very high. This may be due to the presence of a calcification in this area. In slice 1, part of the inner and outer edges has been extracted. We can guess these contours in slice 2 although the stent intensity is very smoothed. The visual distinction stent / lumen is not easy. This may be due either to an excessive protuberance of the vascular wall (intimal hyperplasia), which creates a hypo-dense area inside the stent or to a image resolution problem. The situation appears analogous in slice 5.

The computational time depends on the complexity of the structures. A volume of size  $40 \times 40 \times 100$  can be processed within 10 minutes against about 3 minutes for 100 slices  $30 \times 30$ .

#### 4. Conclusion

We applied a level set approach to refine the contour extraction in presence of severe pathologies: calcified zone, calcified aneurysm, stenosis. Difficulties remain nevertheless inherent in the size of the object such as very thin calcification or narrow stenosis. A further extension will be to introduce statistical models to improve the extraction for these objects.

#### References

- [1] Larralde A., Boldak C., Garreau M., Toumoulin C., D. Boulmier, Y. Rolland: "Evaluation of a 3D segmentation software for the coronary characterization in Multi-Slice Computed Tomography", Second International Workshop on Functional Imaging and Modeling of the Heart, FIMH'03, June 5-6, 2003, Lyon, France.
- [2] Boldak C., Rolland Y., Toumoulin C., Coatrieux J.L.: "An improved model-based vessel tracking algorithm with application to Computed Tomography Angiography"; Journal of "Biocybernetics and Biomédical Engineering", vol 3 (1), 2003, pp 41-64.
- [3] Osher S., Sethian J.A: "front propagating with curvature dependent speed: algorithm based on Hamilton-Jacobi formulation", Journal of Computational Physics, 79, (1988), pp 12-49
- [4] Malladi R., Sethian J.A, Vemuri B.C.: "Shape modelling with front propagation: a level set approach", IEEE Transaction on Pattern Analysis and Machine Intelligence, 17(2), (1995), pp 158-174